Extended Abstracts of the 2008 International Conference on Solid State Devices and Materials, Tsukuba, 2008, pp. 690-691

A-6-3

Formation of Low Resistive S/D-Extension using Carborane Molecular Ion Implantation for Sub-45-nm PMOSFET

S. Endo, Y. Kawasaki, T. Yamashita, H. Oda, and Y. Inoue

Production Technology Development Div., Renesas Technology Corp.
4-1, Mizuhara, Itami, Hyogo, 664-0005, Japan
Phone: +81-72-787-2379 E-mail: endo.seiichi@renesas.com

1. Introduction

For further CMOS scaling, an introduction of a high-k/metal stack or stress induced carrier mobility enhancement is extensively studied. In addition, controlling short-channel effects is required to take full advantage of these techniques. An obvious way to minimize the short-channel effects is a use of ultra shallow source/drain extension (SDE). However, simple reduction of the SDE depth causes the increase of parasitic resistance and degrades the device performance. Therefore, formation of ultra shallow SDE with sufficiently low resistance is a key to realize high-performance MOSFETs for 45-nm node and beyond. As for the boron doping technology, cluster ion implantation [1-2] has been studied as a replacement for conventional sub-keV ion implantation. Recently, carborane ($C_2B_{10}H_{12}$) molecular ion implantation is also reported to form a p-type ultra shallow junction [3].

In this work, carborane molecular ion implantation and advanced annealing using spike-RTA and laser spike annealing (LSA) were applied for SDE of 45-nm pMOSFETs. Advantage of carborane molecular ion implantation to B^+ ion implantation is discussed from the view point of transistor performance.

2. Experimental

Fig. 1 schematically shows a process flow in this study. Carborane molecular ion implantation is simply replaced with boron ion implantation for SDE formation in the conventional process flow. The acceleration voltage of carborane molecular was 2.0 keV and the dosage was $3x10^{13}$ cm^{-2}. As a reference, 0.2 keV and $3x10^{14}$ cm^{-2} B^+ ion implantation was also implemented. Activation annealing was accomplished after SDE implantation and B^+ implantation for deep source/drain (S/D) implantation using combination of spike-RTA and LSA [4].

3. Results and Discussions

(A) Sheet Resistance and Junction Depth

Fig.2 shows cross sectional TEM images for (a) B^+ ions and (b) carborane molecular ions in as-implanted wafers. Si substrate is amorphized from surface to the depth of about 2 nm after carborane molecular ion implantation, while Si wafer is not amorphized after B^+ ion implantation.

Fig. 3 shows as-implanted boron profiles for B^+ ions and carborane molecular ions. It is found that carborane molecular ion implantation produces steep profile without tail distribution which is observed for B^+ ion implantation due to channeling and/or energy contamination. Fig. 4 shows boron profiles after annealing. Fig. 4(a) says that the junction depth of carborane molecular ions is deeper than that of B^+ ions slightly unlike a case of as-implanted. It is considered that TED (transient enhanced diffusion) of boron is enhanced in the case of carborane molecular ions by a lot of residual defects which are generated by molecular ion implantation. Fig. 4(b) shows that the higher the temperature of spike-RTA, the deeper the profile of boron becomes.

Fig. 5 shows the dependence of sheet resistance on the laser power of LSA. Although the difference of junction depth between B^+ ions and carborane molecular ions is not significant, carborane molecular ions show about half sheet resistance as compared with reference B^+ ions.

Fig. 6 shows *Xj-Rs* trade-offs. Carborane molecular ions provide lower sheet resistance than B^+ ions when the junction depth is the same. It is considered that a self-amorphizing effect caused by heavy molecular ions improves the activation of boron by LSA.

(B) Transistor Characteristics

Dependence of pMOS threshold voltage on the gate length is shown in Fig. 7. There is no remarkable difference in V_{th}-L_g characteristics between carborane molecular ions and B^+ ions because of the small difference of the junction depth.

Fig. 8 shows I_{on}-I_{off} characteristics at –1.1-V supply voltage. Carborane molecular ion implantation shows 6% improvement of on-current due to the reduction of the parasitic resistance.

Fig. 9 shows NBTI induced Vt shift. The change of Vt for carborane ions and B^+ ions are almost the same.

4. Conclusions

Boron doping using carborane molecular ion implantation is implemented for formation of S/D-extension of 45-nm pMOSFETs. As compared with B^+ ions, carborane molecular ions show lower sheet resistance for the same junction depth because of its self-amorphizing effect. By simply replacement of B^+ ion implantation with carborane molecular ion implantation, 6% improvement of on-current is obtained for pMOSFETs without noticeable deterioration of short-channel effects. This technology is promising for formation of shallow and low resistance S/D-extensions for 45-nm pMOSFET and beyond.

Acknowledgements

The authors are grateful to Ryuichi Miura, Greg Redinbo, Chris Campbell, Naushad Variam, and Hiroyuki Ito of Varian Semiconductor Equipment Associates, Inc. for carborane molecular ion implantation.

References

[1] K. Goto et al., *IEDM Tech. Dig.* (1996) p.435.
[2] Y. Kawasaki et al., *Nuc. Instr. and Meth in Phys. Res. B 237* (2005) p.25.
[3] A. Renau et al., *IWJT* (2007) p.107.
[4] S. Endo et al., *IWJT* (2007) p.135.

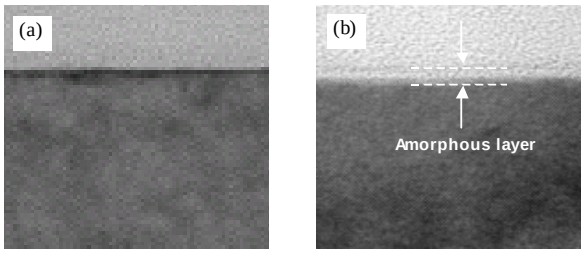

Fig. 2 TEM image of (a) B^+ ions and (b) carborane molecular ions implanted wafers (as-Implant).

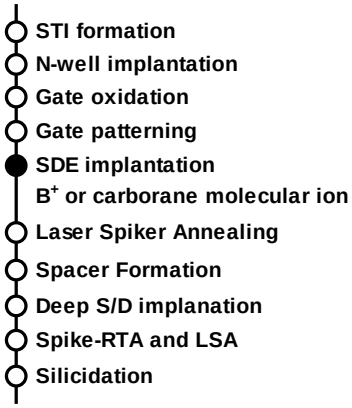

Fig. 1 Process sequence of pMOSFET fabrication.

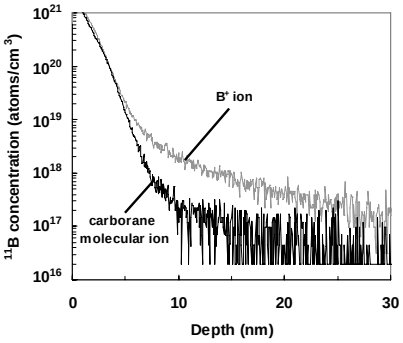

Fig. 3 SIMS profile of ^{11}B by B^+ ions and carborane molecular ions implantation (as-Implant).

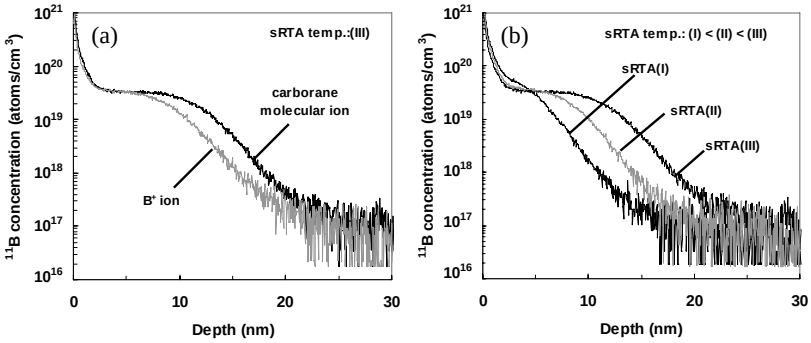

Fig. 4 SIMS profile of ^{11}B by (a) B^+ ions and carborane molecular ions implantation after annealing and (b) carborane molecular ions implantation after annealing by spike-RTA(I)-(III) and LSA.

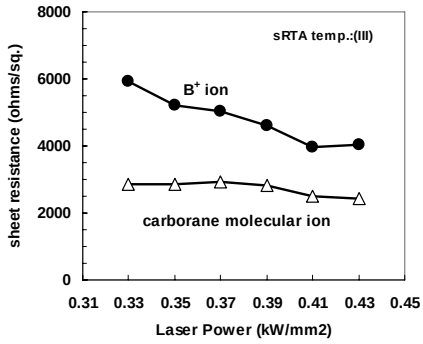

Fig. 5 Dependence of sheet resistance on laser power of LSA.

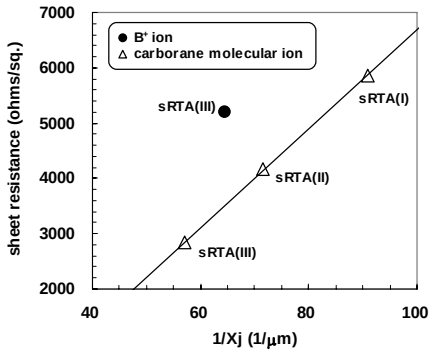

Fig. 6 *Xj-Rs* plot of boron.

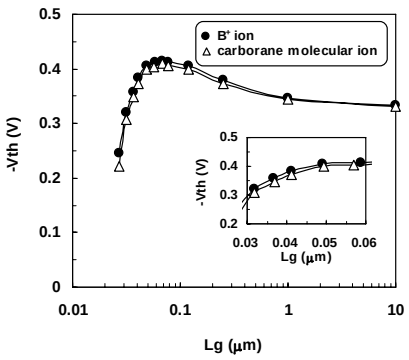

Fig. 7 Roll-off characteristics of PMOSFET.

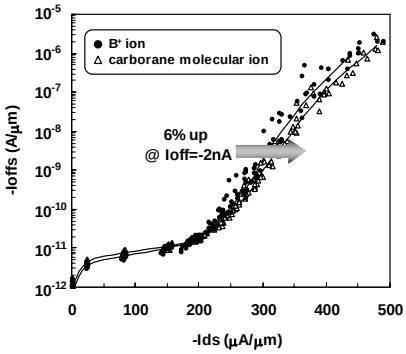

Fig. 8 Ion-Ioff characteristics of PMOSFET.

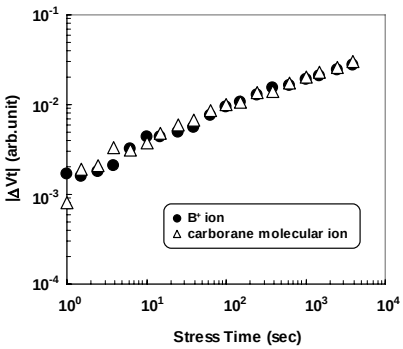

Fig. 9 NBTI induced Vt shift (Stress:Vg=-2.4V, Ta=125°C).